SIMULATION OF AN IMPLANTED PIFA FOR A CARDIAC PACEMAKER WITH EFIELD® FDTD AND HYBRID FDTD-FEM

Introduction

Medical Implanted Communication Service (MICS) has received a lot of attention recently. The MICS is a system which can transmit vital information from an implanted antenna embedded into the human body to external equipment by use of a wireless communication link. Designing antennas for embedded applications is extremely challenging because of reduced antenna efficiency, impact of the environment on the antenna, the need to reduce antenna size, and the very strong effect of multipath losses. Here, a Planar Inverted-F Antenna (PIFA) is employed on the surface of the pacemaker and simulated. The PIFA is designed to operate in the 400 MHz MICS band.

The FDTD method is suitable for microstrip antenna design and has been used extensively for bio-electromagnetic simulations. The Efield® time-domain method offers two solver modes, standalone FDTD on a structured Cartesian grid and hybrid FDTD-FEM. The Efield® hybrid FDTD-FEM solver combines FDTD on the structured grid with a FEM solver on unstructured tetrahedral grids. In this way the Efield® hybrid FDTD-FEM solver allows local spatial refinement of the unstructured grids to resolve geometrical details or to model field singularities near sharp corners, edges or points. Stability is guaranteed through a careful design of the coupling of the FDTD and FEM regions.

The purpose of this application note is to demonstrate the usefulness of the Efield® FDTD and Efield® hybrid FDTD-FEM methods in bio-electromagnetic simulations.

The implanted PIFA

Figure 1 shows a configuration of the pacemaker and the PIFA model. The pacemaker is modelled as a perfect conducting box of size 40x30x10 mm^3. The PIFA is located on the surface of the pacemaker which serves as the counterpoise (ground plane). The antenna element is located in between the two substrate layers. The dimension of the antenna element is 30x20 mm^2 with the operating frequency at the 400 MHz MICS band. The antenna element is fed at the right edge and shorted near the feeding point in order to make the element matched to 50 Ω in human tissue.

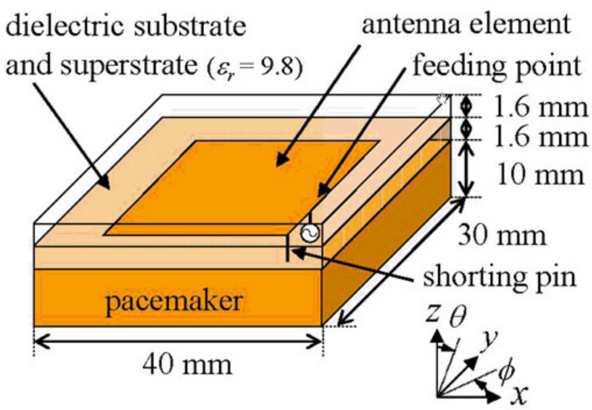

Figure 1: The antenna element placed on top of the pacemaker model

Figure 2 depicts the simulation model configuration when the pacemaker and the PIFA are embedded into the human body. A 2/3 muscle-equivalent phantom is employed as the human model. The distance d between the surface of the pacemaker and the surface of the phantom (d) is fixed to d =6 mm.

Material data:

- Dielectric substrate ε_r=9.8
- Muscle-equivalent phantom ε_r=38.1, σ=0.53 S/m

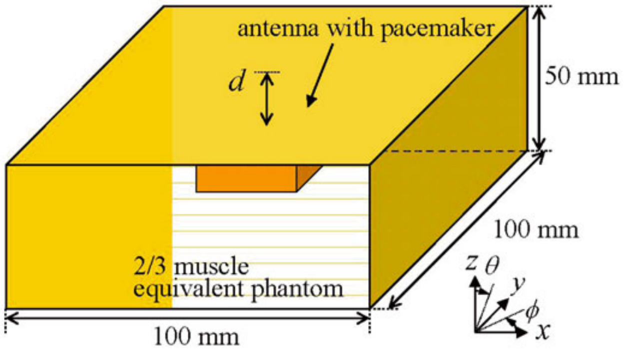

Figure 2: Human tissue equivalent model

FDTD Meshing

Tartan meshing or finite difference meshing is used in Efield® time-domain for standalone FDTD analysis. A finite difference grid is set up, called the lattice, by specifying start and stop coordinates and the cell size for each direction.

The tartan mesh creates "twinkles" or cells (represented by nodes) on vertices, lines, surfaces and bodies. These twinkles can be displayed after meshing. An example of tartan meshing of the pacemaker with the antenna placed inside the muscle phantom is shown in Figures 3 and 4. The lattice edges are shown in the background of Figure 3.

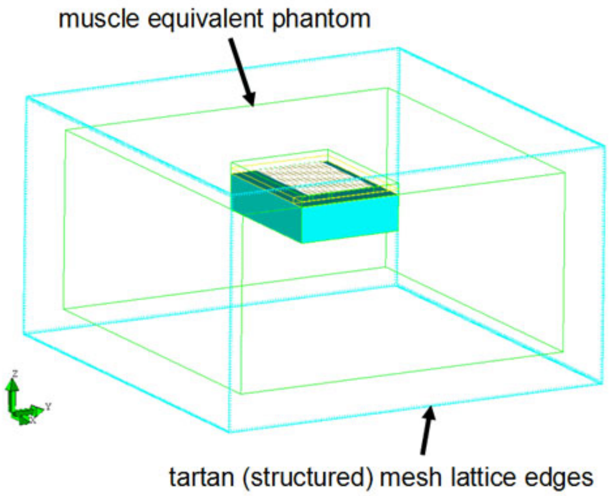

Figure 3: Tartan (FDTD) meshing of the pacemaker with the PIFA placed inside the muscle equivalent phantom

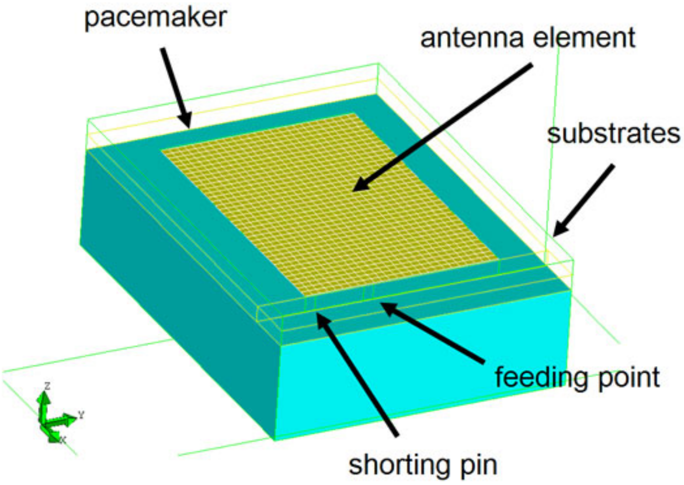

Figure 4: Tartan (FDTD) meshing of the PIFA on the pacemaker

Hybrid FDTD-FEM Meshing

The Efield® hybrid FDTD-FEM solver uses a hybrid mesh which consists of a background tartan mesh with "islands" of unstructured mesh. There are two important concepts in hybrid meshing:

- Cavity - the region to be filled with an unstructured FEM mesh using tetrahedral and triangular elements
- Seed geometry - the geometry upon which a FEM mesh is to be imposed

Hybrid meshing is a combination of tartan and Delaunay meshing. The model is first tartan meshed, after this stage the tartan mesh around the seed geometry is removed and replaced by a tetrahedral mesh, which joins up with the tartan mesh at the boundaries of the cavity. The tetrahedral mesh inside the cavity can be finer than the tartan mesh it replaces and hybrid meshing thus allows certain parts of the mesh to better resolve small details than the rest of the mesh.

The important steps in creating a hybrid mesh are:

- Identify the seed geometry for which an unstructured mesh should be used. The cavities are created around the seed geometry.
- Any entities which happen to occur in a cavity, but which are not seed entities, are known as join entities because they join the seed geometry to the surrounding tartan mesh.
- The outermost layer of tetrahedral elements in the cavity is known as the transition layer. The tetrahedral elements in this layer fit exactly into lattice cells enabling an accurate coupling from the tetrahedral elements to the tartan lattice.

In order to ensure a smooth transition between the unstructured region and the tartan mesh a cavity depth is specified denoting the distance in cells between the seed geometry and the transition layer. Typically a few cells are sufficient.

An Efield® hybrid FDTD-FEM model of the pacemaker with the antenna placed inside the muscle phantom is shown in Figures 5 and 6. Notice that the pacemaker with the antenna element is placed completely inside the cavity and will be meshed using tetrahedral elements. The cavity will cut the upper surface of the muscle equivalent phantom box so the box will partly be meshed using a tetrahedral mesh and the rest of the box using a tartan mesh.

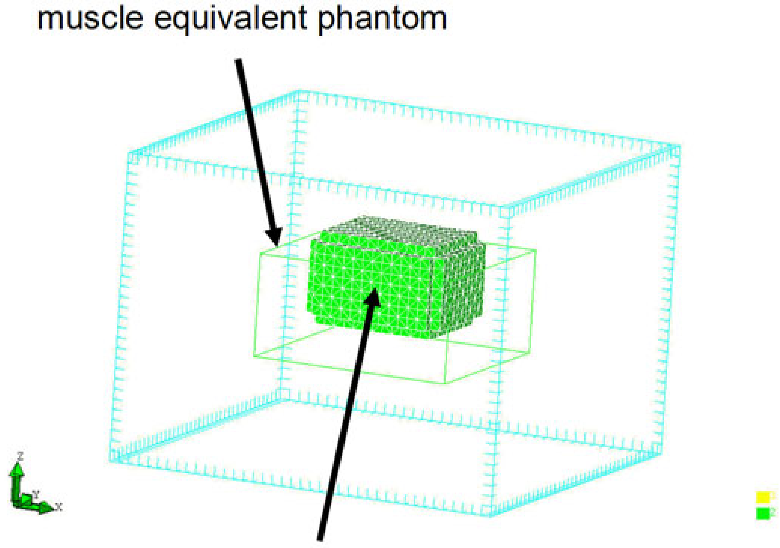

Figure 5: Hybrid (FDTD-FEM) meshing of the pacemaker with the PIFA placed inside the muscle equivalent phantom

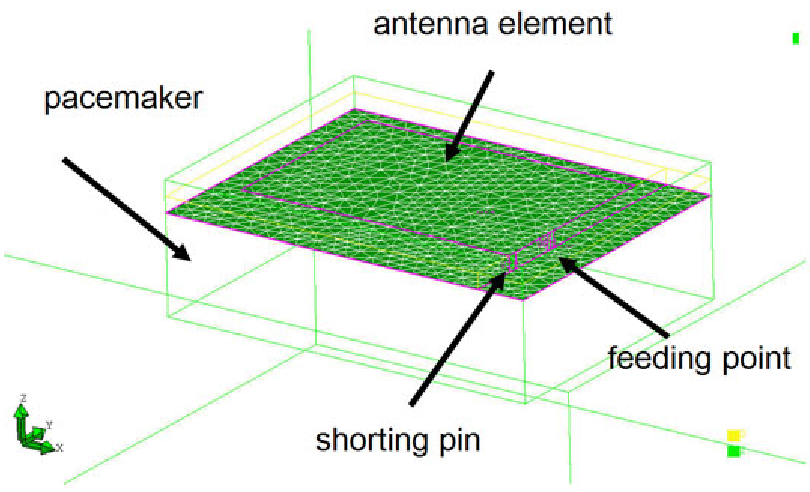

Figure 6: Meshing of the PIFA and pacemaker using the unstructured FEM mesh

Efield® TD Workflow

Figure 7 illustrates the workflow when using the EfieldTD EM GUI. The first task is to sett up Computational Parameters and work downwards. It is always possible to go back to a previous task and modify the values.

- The green boxes in Figure 7 indicate tasks that should always be entered (not necessarily changing the values).
- The blue boxes indicate tasks for specifying geometry. Depending on the problem they may or may not be necessary to enter.
- The yellow boxes indicate functionality tasks that may be used for excitation. In most cases there is only one excitation source but there may be many passive elements (registration ports, wires or lumped circuits).
- The cyan boxes indicate results computations and definitions. Near to far-field computation is optional.

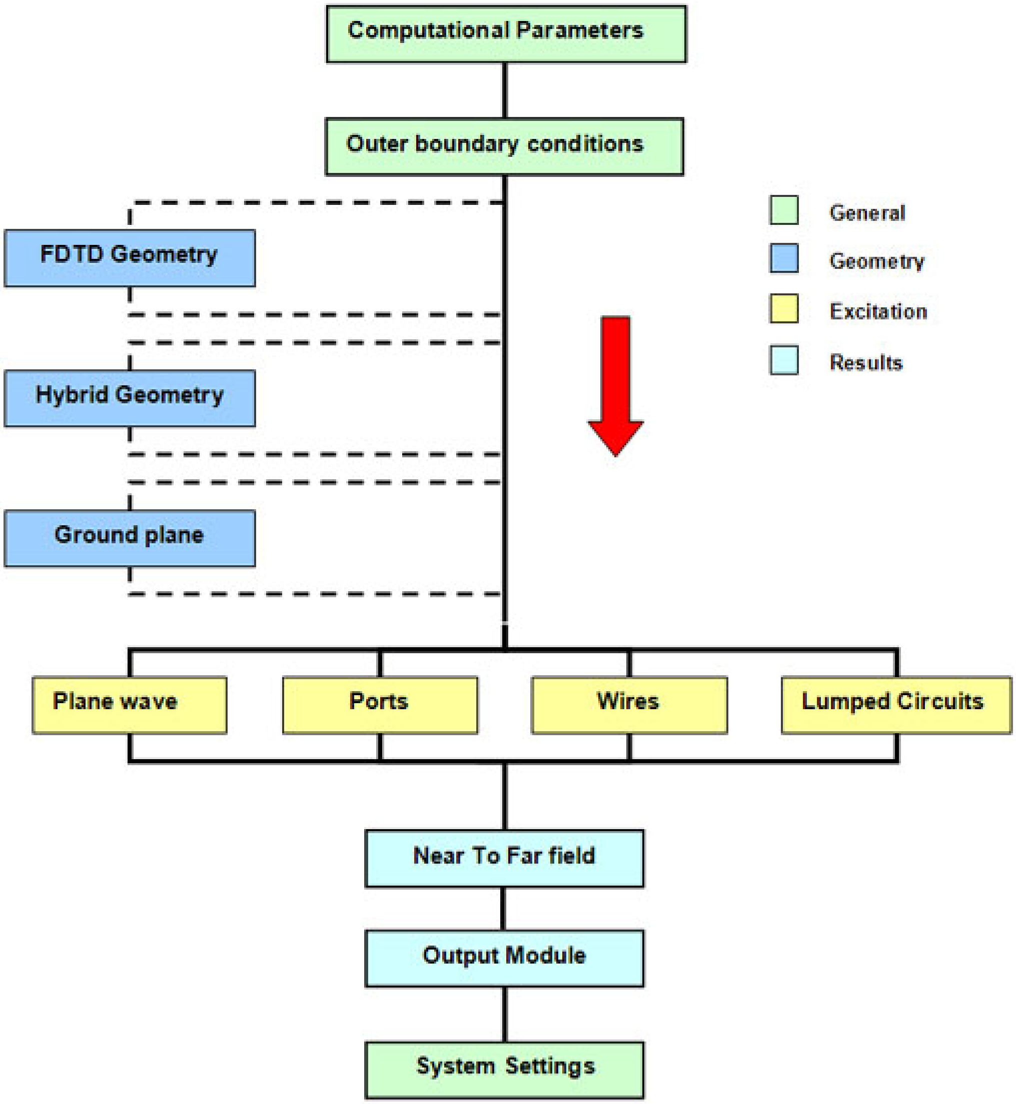

Figure 7: Efield TD EM GUI Workflow

Computations

The problem was solved using both the Efield® FDTD and the Efield® hybrid FDTD-FEM solver. Two different FDTD models, "fdtd1" and "fdtd2", with 1.6 mm and 0.8 mm cellsize respectively were simulated. Three different hybrid FDTD-FEM models were used, "fem1", "fem2" and "fem3". Data for all simulations is given in Table 1 and 2.

Table 1: Simulations with 1 processor on an AMD Dual Core Opteron 285 2.6 GHz with 16 Gb memory.

Model	Solver	Cell size [mm]	Nodes (FDTD)	Nodes (FEM)	Elements (FEM)	Time step [10^{-12} s]	Time steps N	Time [min]
"fdtd1"	FDTD	1.6	358200	-	-	2.77	20000	80
"fdtd2"	FDTD	0.8	1745000	-	-	1.38	40000	290
"fem1"	FDTD-FEM	5	48000	10753	37194	8.66	6500	52
"fem2"	FDTD-FEM	4	66825	14675	35467	6.93	8000	53
"fem3"	FDTD-FEM	1.6	358200	135815	62846	2.77	20000	161

Table 2: Simulations with 2 processors on an AMD Dual Core Opteron 285 2.6 GHz with 16 Gb memory.

Model	Solver	Cell size [mm]	Time step [10^{-12} s]	Time steps N	Time (scalar) [minutes]	Time (2 processors) [min]
"fdtd1"	FDTD	1.6	2.77	20000	80	28
"fdtd2"	FDTD	0.8	1.38	40000	290	156
"fem1"	FDTD-FEM	5.0	8.66	6500	52	20
"fem2"	FDTD-FEM	4.0	6.93	8000	53	58
"fem3"	FDTD-FEM	1.6	2.77	20000	161	117

Approximate timing data for simulation on an AMD Dual Core Opteron 285 workstation with one or two processors is given in Table 2.

The outer boundary condition was set to "perfectly matched layer" for the six boundary surfaces of the computational domain. The perfectly matched layer absorbing boundary condition has 8 layers in this particular case with a theoretical reflection of 0.01%. The user can choose the number of layers in order to adjust the computational effort to what is actually needed depending on the actual simulation problem.

Consider a cubic FDTD cell with *dx=dy=dz=d*. The Courant stability condition will limit the maximal possible time step *dt*

$$dt = CFL \cdot \frac{d}{c\sqrt{3}}$$

where

$$CFL \leq 1$$

and *c* is the wave propagation speed. The *CFL* number used in the simulations was 0.9.

The maximal possible time step *dt* is proportional to the cell size and will be reduced when the FDTD cell size is small and thus the number of time steps needed for a convergent solution will increase. Notice that a fine FEM mesh can be combined with a relatively coarse FDTD mesh. The number of time steps needed for convergence is then lower than for a highly resolved standalone FDTD simulation.

Excitation

The excitation in this example was a lumped circuit voltage source with inner resistance 50 Ω. A lumped(TD) material was used to define the voltage source. The lumped circuit model is a discrete model which assumes no variations in the current and voltage over the circuit geometry. It may be assigned either to a surface or a line entirely located in the FDTD region or to a line in the FEM region. See Figure 8 for a detail of the meshed antenna in FEM whit the lumped voltage source placed on a line. A resistive load defined on a lumped circuit source is interpreted as an inner source resistance in the simulation which will speed up the convergence. The correct antenna impedance (and reflection) related to the characteristic impedance will be calculated in the simulation.

A number of different wave forms are available. A modulated Gauss pulse was used for the pulse excitation. When using modulated Gaussian pulse the user specifies a frequency interval by setting the start and end frequency.

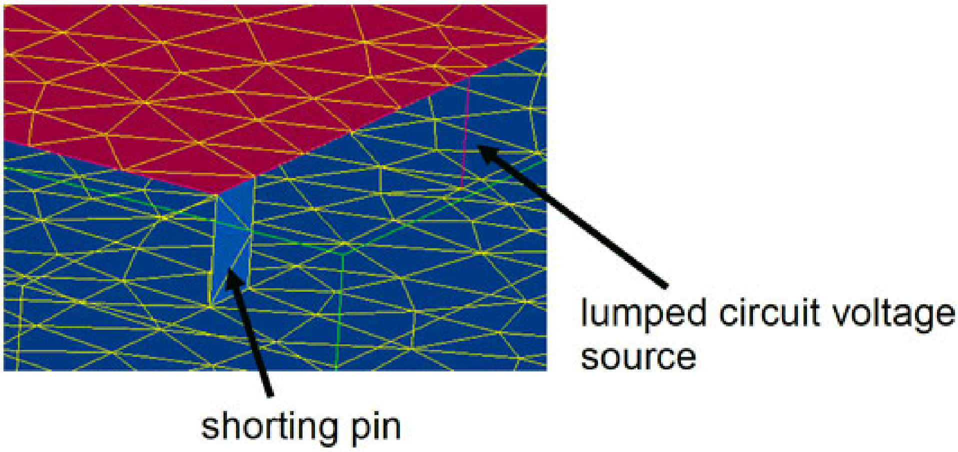

Figure 8: The lumped circuit element excitation in FEM. The lumped circuit voltage source is placed on a line of the model

Impedance & Return Loss

Simulated real and imaginary parts of the impedance are plotted in Figure 9 for the different Efield® FDTD and Efield® hybrid FDTD-FEM models.

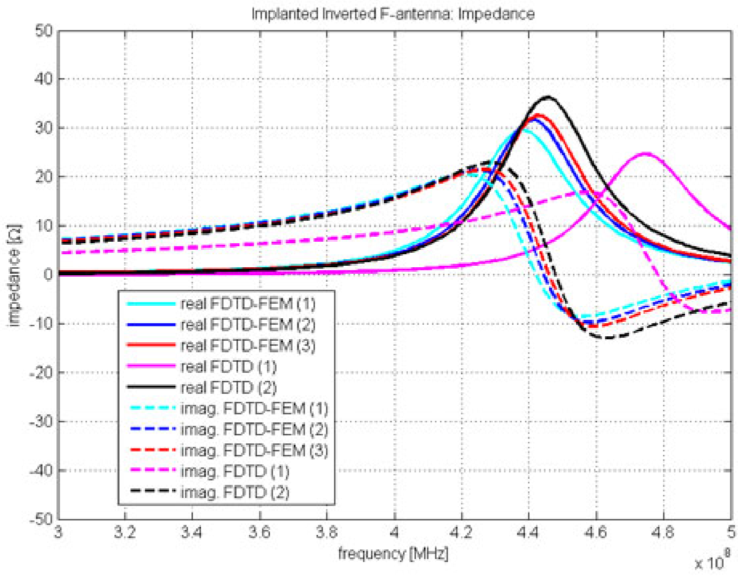

Figure 9: Real and imaginary parts of the impedance

The simulated return loss for the PIFA is presented in Figure 10. The 1.6 mm FDTD model ("fdtd1") is too coarse but the 0.8 mm FDTD model ("fdtd2") is in reasonably good agreement with the three FDTD-FEM models with different mesh refinement.

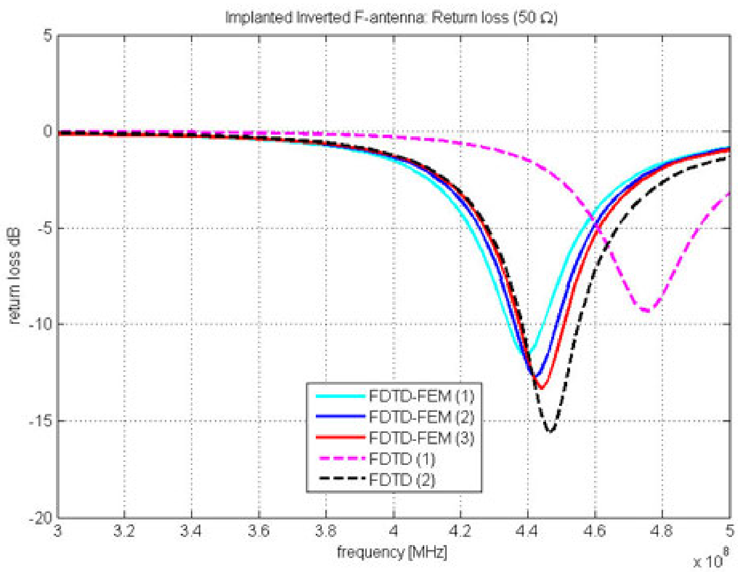

Figure 10: Return loss of the PIFA

FDTD Far-field & Currents

The Efield® Result Manager provides tools for assessing results from EfieldTD including model visualisation, results presentation, model and result verification, and data manipulation functions. A number of different options are available in the Efield® Result Manager for presenting far-field results. A 3D far-field plot ("fdtd2") is shown in Figure 11.

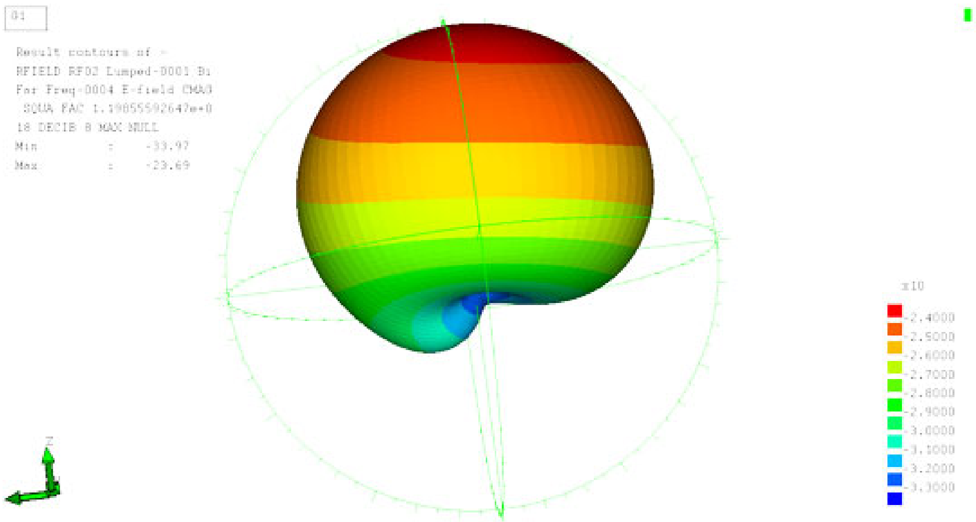

Figure 11: 3D far-field plot of the implanted PIFA

Results can be presented as contours of constant value by using either the node based or element-based result data from the Efield® results database. Surface currents on the antenna element and the pacemaker are displayed in Figure 12. The tartan contours option presents the results as the filled contours on tartan twinkles.

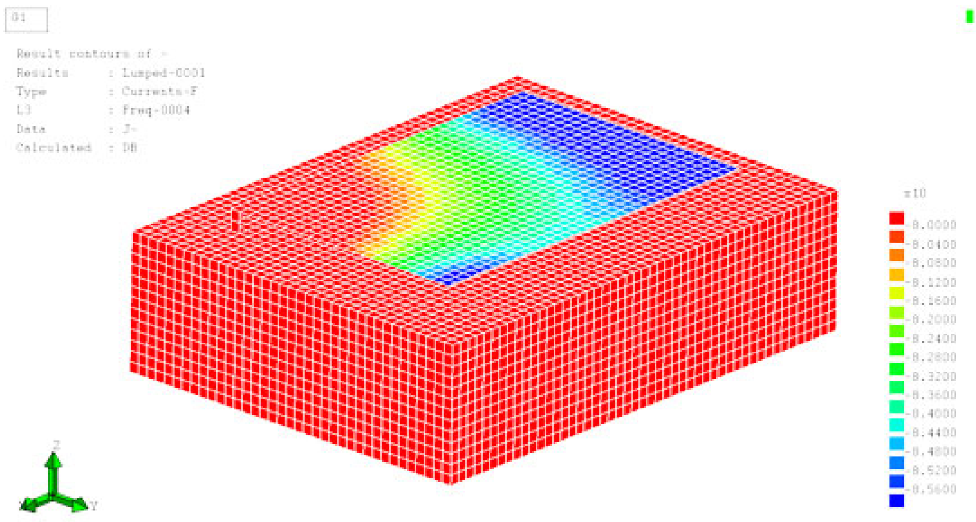

Figure 12: Surface currents on a structured mesh

FDTD-FEM Far-field & Currents

Result visualisation in Efield® hybrid FDTD-FEM is similar to Efield® FDTD visualisation. A 3D far-field plot ("fem3") is shown in Figure 13. Surface currents on the antenna element and the pacemaker are displayed in Figure 14. Contour plots are displayed as filled contours for results based on unstructured geometry, such as surface currents located in the unstructured region.

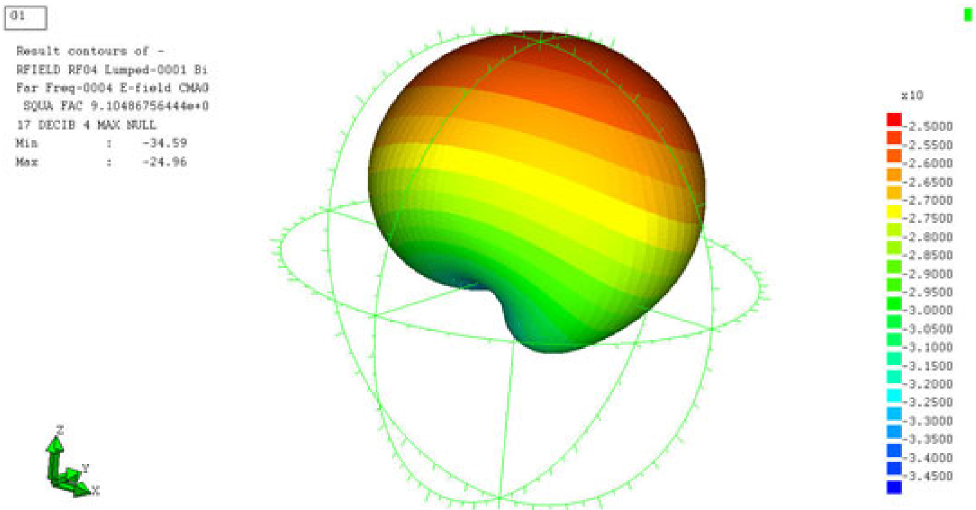

Figure 13: 3D far-field plot of the implanted PIFA

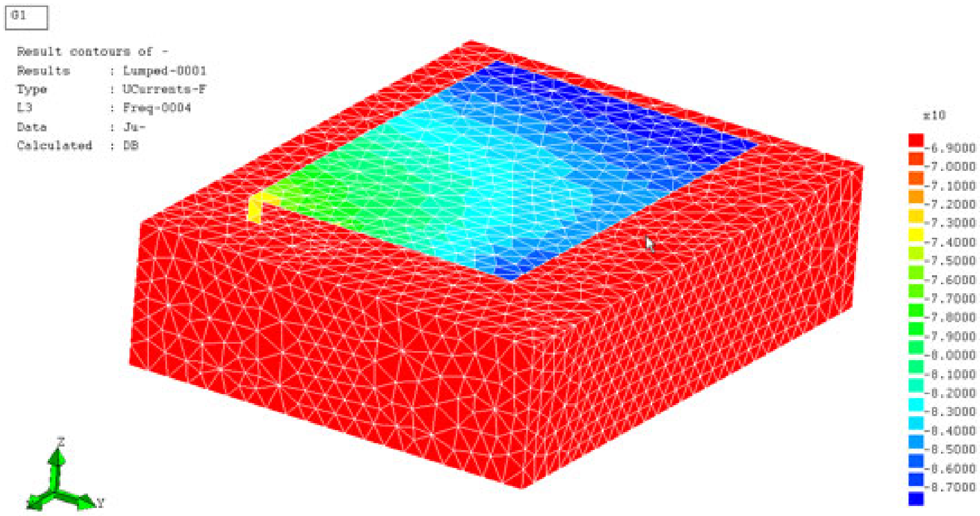

Figure 14: Surface currents on an unstructured mesh

Conclusions

The Efield® FDTD solver is multi-block parallelized on a Cartesian grid. Functionality includes waveguide ports, voltage and current sources, S-parameter computation and a range of far-field transforms which makes the Efield® FDTD method well suited for broadband analysis of microwave and antenna problems.

The Efield® hybrid FDTD-FEM solver combines a parallel FDTD solver on Cartesian grids with a FEM solver on unstructured grids. The underlying philosophy of the hybrid approach is to take advantage of the strengths of the individual solvers without suffering from their weaknesses. The FEM solver enables accurate modeling of complex geometries through the use of body-conforming unstructured grids.

The hybrid solver allows local spatial refinement of the unstructured grid to resolve geometrical details or to model field singularities near sharp corners, edges or points. Stability is guaranteed through a careful design of the coupling of the FDTD and FEM solvers.

It is in general possible to use a larger time step if a local spatial refinement is combined with a coarser structured grid. The number of time steps needed for convergence is then substantially reduced compared to a highly resolved standalone FDTD simulation. The examples presented in this application note show reduced simulation time with Efield® hybrid FDTD-FEM method compared to standalone FDTD at the same accuracy.

The Efield® FDTD and hybrid FDTD-FEM solvers are parallelized using MPI multi-block technique. Both solvers have excellent parallel scaling properties as demonstrated in the examples presented here and will utilize available hardware resources in an optimal way.

The Efield® time-domain solvers can handle a wide variety of materials as

- Dielectric and magnetic materials with electric and magnetic losses
- Dispersive material based on a recursive convolution model
    - Debye model
    - Lorentz model
    - General dispersive material

making the Efield® FDTD and Efield® hybrid FDTD-FEM methods useful in bio-electromagnetic simulations.

The Efield® FDTD and Efield® hybrid FDTD-FEM solvers produce accurate results. The simulation result of the cardiac PIFA placed inside the muscle equivalent phantom is in good agreement with measurement result (not presented here). See ref. [1].

References

[1] Tamotsu Houzen, Masaharu Takahashi, Kazuyuki Saito, and Koichi Ito, “Implanted Planar Inverted F-Antenna for Cardiac Pacemaker System”, Proceedings of iWAT2008, Chiba, Japan (2008).

Efield AB, Skalholtsgatan 10 B,
SE-164 40 Kista, Sweden
Tel: +46 8 410 03 510
Email: contact@efieldsolutions.com
www.efieldsolutions.com

